Received May 13, 2020, accepted May 21, 2020, date of publication May 28, 2020, date of current version June 9, 2020.

Digital Object Identifier 10.1109/ACCESS.2020.2998177

Carrier-Based Discontinuous PWM Method for Five-Leg Inverter

JUNE-HEE LEE[1], (Member, IEEE), JUNE-SEOK LEE[2], (Member, IEEE), AND JOON-HYOUNG RYU[1], (Member, IEEE)

[1]Korea Railroad Research Institute, Uiwang 16105, South Korea
[2]School of Electronics and Electrical Engineering, Dankook University, Yongin 16890, South Korea

Corresponding author: June-Seok Lee (ljs@dankook.ac.kr)

This work was supported by the Railroad Technology Research Program through the Ministry of Land, Infrastructure and Transport of Korean Government under Grant 20RTRP-B146008-03.

ABSTRACT This paper proposes a rotation carrier-based discontinuous pulse width modulation (CB-DPWM) method for the five-leg inverter (FLI). The FLI based on two-level topology consists of 10 switching devices for driving dual motors. Therefore, two switching devices can be reduced to compare the configuration using two three-leg inverters for driving dual motors. The proposed pulse width modulation (PWM) method is based on the reference signals which are used in existing carrier-based continuous pulse width modulation (CB-CPWM) method for FLI. In the proposed rotation CB-DPWM method, one of five-leg is periodically clamped to $V_{dc}/2$ or $-V_{dc}/2$ by adding the offset voltage to the reference voltages of the existing CB-CPWM method. The five reference voltages for all legs are considered to calculate the offset voltage of the proposed rotation CB-DPWM method. Consequently, since the proposed rotation CB-DPWM method has less switching than the existing CB-CPWM, the switching loss can be reduced and it results in the efficiency improvement. Simulation and experimental results confirm the effectiveness and feasibility of the proposed method.

INDEX TERMS Five-leg inverter (FLI), modulation, rotation carrier-based discontinuous pulse width modulation (CB-DPWM), dual-motor driving system.

I. INTRODUCTION

The dual motor drive systems (DMDSs) are widely used in many industrial fields such as propulsion system, ventilation system, textile, paper manufacturing, conveyer system and so on, and they have proved to be reliable and inexpensive. Generally, each motor of DMDSs requires a three phase voltage source inverter (VSI) for driving them independently, and two inverters share a common DC-link input voltage; therefore, a total of twelve switches are required. Recently, DMDSs have been researched for saving space and cost, and reducing power losses. Reducing the number of switching devices is desirable; therefore, many research results have shown simplified configurations for DMDSs. For example, a reduced-switch-count inverter [1]–[3], a nine-switch inverter [4]–[7], a mono inverter [8]–[10], a five-leg inverter [11]–[26], and so on.

The five-leg inverter (FLI) has a simple structure among several topologies, and is widely used to independently drive two induction motors. One phase of each three phase motor is connected to the same leg of FLI. The remaining phases of each three phase motor are connected to the remaining legs one by one as shown in Fig. 1. Therefore, FLI can save two switching devices compared with the dual three-leg inverter system. Mostly the reference voltages of the common leg for two induction motors are individual, as a result, the conventional PWM method cannot be applied directly for FLI because the common leg does not satisfy the control requirements of two induction motors. In order to overcome this drawback, however, many studies have suggested PWM methods for FLI such as the carrier-based sinusoidal PWM (CB-SPWM) and the carrier-based space vector PWM (CB-SVPWM).

There are several control methods for driving dual motors using FLI [11]–[26]. The similarity of these control methods is that the sum of the output voltages supplied to the dual motors is limited to the DC-link voltage. In addition, the switching devices of the common leg must withstand up to twice the current of the other leg. In this case, the different switching devices should be used for the

The associate editor coordinating the review of this manuscript and approving it for publication was Zhilei Yao.

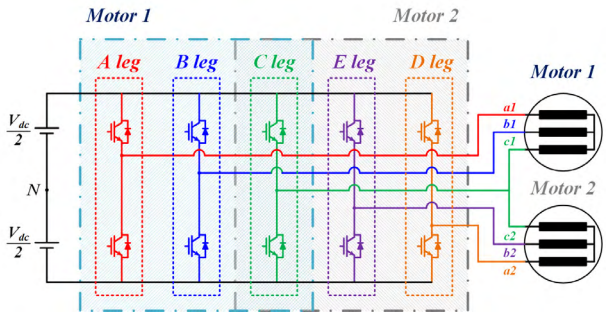

FIGURE 1. Five-leg inverter system with two induction motors.

common, or the capacity of the FLI should be used only 50%. Reference [24] has been studied to overcome this drawback. This advanced speed control method is suitable for maintaining constant speed regardless of any load conditions. Furthermore, the maximum value of common leg current is always smaller than that of the other leg due to the angle controller which keeps the current phase difference of two induction motors connected to the common leg to 180 degrees. Therefore, it is not necessary to increase the switching device rating characteristic of common leg. The advanced control method can be effectively used in many industrial fields such as air conditioning system in railway or vehicle, dual cement kiln drive, conveyor belts and so on [38]–[40]. In this case, the FLI driving two motors independently can be used most efficiently when the two motors operate at the same speed, and the electrical phase difference between the two motors is controlled to 180 degrees. Therefore, the advanced control is applied as the control method of this paper.

This paper proposes a rotation carrier based discontinuous PWM (CB-DPWM) method to increase the system efficiency. The CB-DPWM method has been well-known for the switching loss reduction of switching device. The CB-DPWM method leads the switching devices operation in only two of three legs. The discontinuous modulation section without switching can be set up to 120 degrees of the fundamental period of the reference voltage in three-leg inverter [27]–[37]. However, the PWM methods introduced in many papers related to FLI are typical continuous modulation schemes in which all switching devices always operates. Especially, [36] and [37] introduce various DPWM methods applied to FLI. Both papers implement various DPWM methods using the space vector modulation (SVM) method and analyze the characteristics of various DPWM methods. In general, SVM method requires a lot of computation time to apply the micro-controller unit (MCU). SVM method has to select the switching vector corresponding to the reference voltage from the vector table and calculate the dwelling time for every control period. However, many studies have found modulation methods that can have the same effect as SVM method when an appropriate offset voltage is applied to the CB-SPWM method [41]–[43]. In addition, DPWMMAX, which clamps the reference voltage to $0.5V_{dc}$, and DPWMMIN, which clamps to $-0.5V_{dc}$, increase conduction loss to one of the two switches in the half-bridge leg. It leads to thermal unbalance between legs. In [37], various DPWM methods were implemented and analyzed based on the space vector modulation method for a five phase induction motor. The shift of five-phase induction motor between each phase voltage is $72(=2\pi/5)$ degrees. Among the various DPWM methods introduced in [37], DPWM1 method applies DPWMMAX and DPWMMIN alternately to the reference voltage every 36 degrees. However, DPWM1 method in [37] is not suitable for driving dual motor system using the advanced speed control method because the shift of five phase voltages is not fixed at 72 degrees. To overcome these drawbacks, this paper proposes a rotation CB-DPWM method. The proposed rotation CB-DPWM method simply implements the DPWM method using the carrier-based modulation method with the offset voltage. Using the proposed method, the computation time can be shorter than that of SVM method. In addition, the proposed rotation CB-DPWM method alternately applies the offset voltage for DPWM method every reference voltage period. Therefore, it is possible to increase the system efficiency and balance the loss of the switching devices. The simulation and experimental results are implemented to confirm the feasibility of the proposed method.

II. DESCRIPTION OF FLI AND CONTROL METHOD

A. FIVE-LEG INVERTER

Fig. 1 shows the main circuit of the FLI with the two induction motors. The FLI consists of five legs with ten switching devices, a DC-link source (V_{dc}), and two induction motors, respectively. The leg A and B are connected directly to phases $a1$ and $b1$ of the induction motor 1 ($IM1$), respectively. Similarly, the leg D and E are connected directly to phases $a2$ and $b2$ of the induction motor 2 ($IM2$), respectively. As a result, there is a common leg C, which is shared by both phase $c1$ of $IM1$ and phase $c2$ of $IM2$. It is possible to reduce the number of switching devices and simplify the circuit structure compared with conventional configuration consisting two three-leg inverters.

B. ADVANCED SPEED CONTROL METHOD

In general, when two induction motors connected to FLI are driven in synchronization, the maximum current of the common leg flows up to twice the other leg current. The maximum current ($I_{c,peak}$) of the common leg considering the load condition is expressed as

$$I_{c,peak} = \sqrt{i_{c,m1}^2 + i_{c,m2}^2 + 2i_{c,m1}i_{c,m2}\cos(\alpha)}. \quad (1)$$

where $i_{c,m1}$ and $i_{c,m2}$ are the C-phase current of two induction motors, and α represents the angle between $i_{c,m1}$ and $i_{c,m2}$, respectively. As shown in (1), if α is to be zero, the magnitude of the common leg current is twice as large as that of other legs. To overcome this drawback, therefore, [24] proposes two control schemes.

1) The angle controller in [24] minimizes $I_{c,peak}$ of FLI by maintaining the rotor flux angle difference between two induction motors in reverse.
2) The slip controller in [24] maintains the same speed of both induction motors regardless of the load conditions.

Fig. 2 shows the simplified control block diagram of the advanced speed controller proposed in [24]. $T_{m1,load}$ and $T_{m2,load}$ represent the load torque condition of each motor, $\omega_{r,m1}$ and $\omega_{r,m2}$ represent the speed of each motor, θ_{m1} and θ_{m2} represent the electrical angle of each motor, $\omega^*_{r,m1}$ and $\omega^*_{r,m2}$ represent the reference speed of each motor, I^*_{dqen} (n = 1, 2) represents the d-q axis reference current, I_{dqen} (n = 1, 2) represents the d-q axis current, $I^*_{den,r}$ (n = 1, 2) represents the d axis rated reference current, $I^*_{den,c}$ (n = 1, 2) represents the output of the slip controller, and S_x (x = a, b, c, d, e) represents the gate signal, respectively. First, the load torques of two induction motors are compared. Next, the induction motor with a larger load torque is driven by speed controller. At this time, the speed of the other induction motor is synchronized with the speed of the induction motor having a large load torque through the slip controller. In addition, the angle controller is used to maintain the rotor flux angle between two induction motors as 180 degrees to minimize the common leg current of FLI.

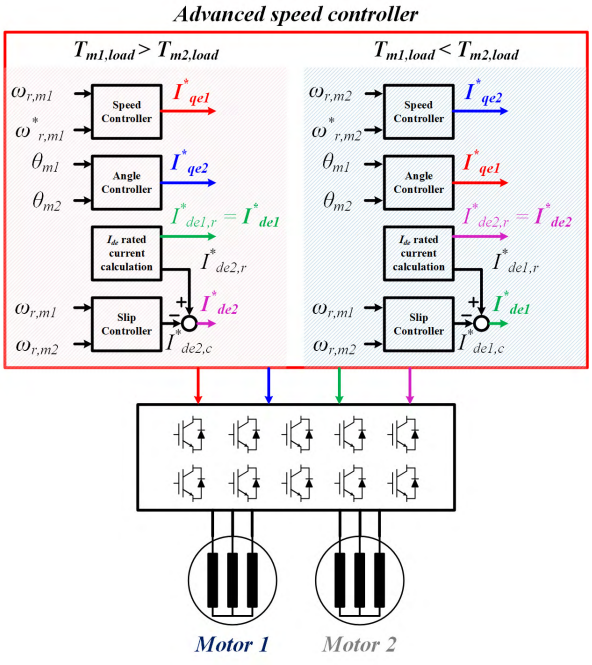

FIGURE 2. Block diagram of advanced control in [24].

III. CB-PWM FOR FLI

The CB-PWM method for FLI has been continuously developed through many studies. Among existing CB-PWM methods for FLI, the double zero sequence (DZS) method used in this paper is the simplest method [11]–[13]. The DZS method uses two offset voltages called as the zero-sequence signals. Fig. 3 shows the modulation scheme using the DZS method.

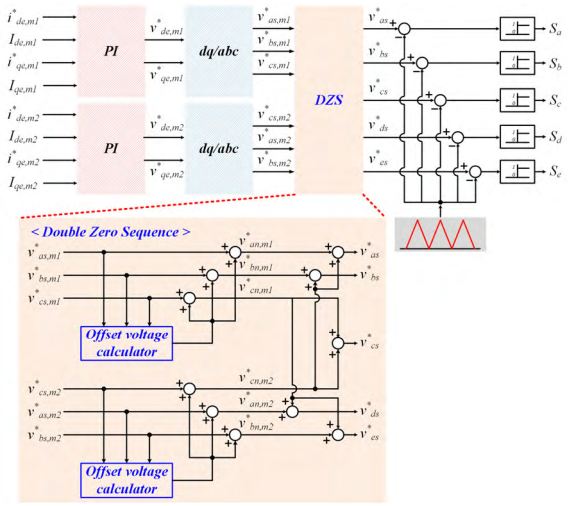

FIGURE 3. Modulation scheme using DZS method.

In general, the pole voltage of inverter is determined by the switching devices on-off state of each phase. The reference voltages ($V^*_{as,n}$, $V^*_{bs,n}$, and $V^*_{cs,n}$) determine the switching devices on-off state of each phase in the CB-PWM method and can be expressed as

$$\begin{aligned} V^*_{as,n}(t) &= \frac{2V_n}{V_{dc}} \sin(2\pi f_n t + \theta_{mn}) \\ V^*_{bs,n}(t) &= \frac{2V_n}{V_{dc}} \sin\left(2\pi f_n t + \theta_{mn} + \frac{2}{3}\pi\right), \quad (\mathrm{n} = 1, 2) \\ V^*_{cs,n}(t) &= \frac{2V_n}{V_{dc}} \sin\left(2\pi f_n t + \theta_{mn} - \frac{2}{3}\pi\right). \end{aligned} \tag{2}$$

where V_n is the pole voltage amplitude and f_n is the frequency of stator electrical speed for *IM1* and *IM2*, respectively. $V^*_{as,n}$, $V^*_{bs,n}$, and $V^*_{cs,n}$ are called as the reference voltage of CB-SPWM method.

To extend the linear region to 1.1547 times wider than the SPWM method [11], the offset voltage ($V_{offset,n}$) is used and calculated as

$$v_{offset,n} = -\frac{V_{\max,n} + V_{\min,n}}{2}, \quad (\mathrm{n} = 1, 2). \tag{3}$$

where $V_{max,n}$ represents the maximum reference voltage and $V_{min,n}$ represents the minimum reference voltage, respectively. Using $V_{offset,n}$, which is first zero-sequence signal of DZS, it is possible to obtain similar results with the third harmonic injection modulation scheme of three-leg inverter. This method is called CB-SVPWM. In the CB-SVPWM, the reference voltages ($V^*_{an,n}$, $V^*_{bn,n}$, and $V^*_{cn,n}$) of each motor are expressed as (4) by adding the $V_{offset,n}$ to (2).

$$\begin{aligned} V^*_{an,n} &= V^*_{as,n} + v_{offset,n} \\ V^*_{bn,n} &= V^*_{bs,n} + v_{offset,n}, \quad (\mathrm{n} = 1, 2) \\ V^*_{cn,n} &= V^*_{cs,n} + v_{offset,n}. \end{aligned} \tag{4}$$

The six reference voltages calculated from (4) should be reduced to five corresponding to the number of inverter legs. The C-phase reference voltage, $V^*_{cn,2}$, is added as an offset voltage to the A- and B-phase reference voltages of *IM1*,

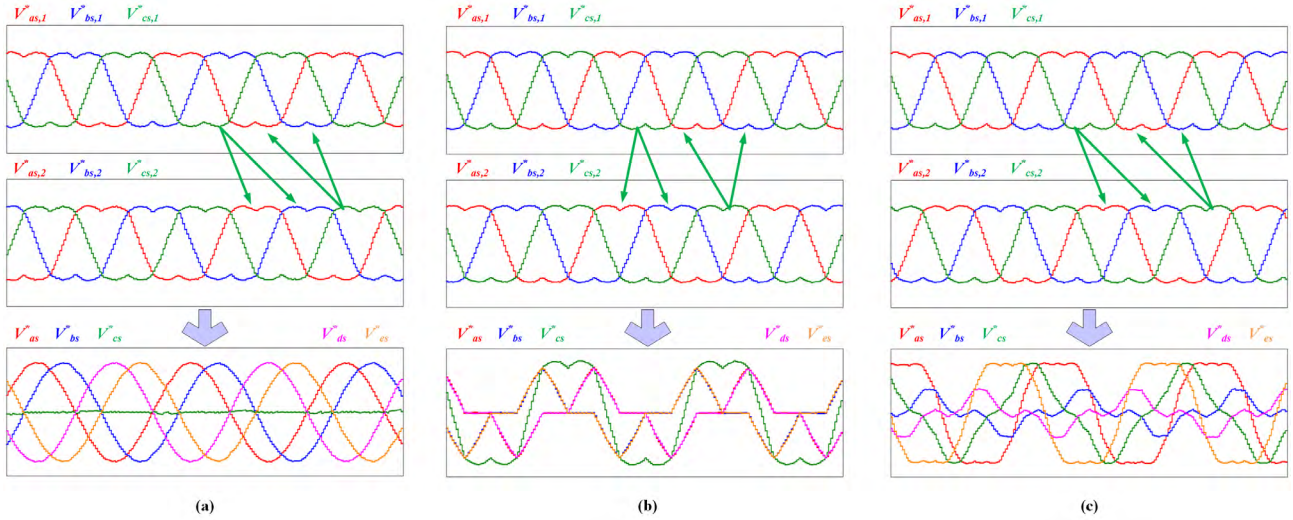

FIGURE 4. Configuration of reference voltage using DZS method. (a) $\alpha = 180°$, (b) $\alpha = 0°$, (c) $\alpha = 90°$.

whereas the C-phase reference voltage, $V^*_{cn,1}$, is added as an offset voltage to the A- and B-phase reference voltages of $IM2$. This offset voltage is a zero-sequence component and does not appear in the line-to-line voltage of each induction motors [11]. Therefore, the final reference voltages (V^*_{as}, V^*_{bs}, V^*_{cs}, V^*_{ds}, and V^*_{es}) for FLI can be expressed as

$$\begin{aligned} V^*_{as} &= V^*_{an,1} + V^*_{cn,2} \\ V^*_{bs} &= V^*_{bn,1} + V^*_{cn,2} \\ V^*_{cs} &= V^*_{cn,1} + V^*_{cn,2} \\ V^*_{ds} &= V^*_{cn,1} + V^*_{an,2} \\ V^*_{es} &= V^*_{cn,1} + V^*_{bn,2}. \end{aligned} \tag{5}$$

Therefore, the FLI operates with the continuous PWM in the linear region, as if both induction motors are driven by independent three-phase inverters. In addition, the available DC-link voltage depends on the magnitude of each reference voltage. For example, if the modulation index ($MI = V^*_{xs}/0.5V_{dc}$, x = a,b,c,d,e) of $IM1$ is 0.4, the maximum MI of $IM2$ is 0.6 [11]. Fig.4 shows the process of generating the final reference voltages according to α. The final reference voltages for the FLI exist in the linear region. In addition, when the advanced speed control method is applied, the final reference voltages of FLI are shown in Fig. 4(a).

IV. PROPOSED ROTATION CB-DPWM FOR FLI

Generally, among the various voltage modulation methods, a CB-CPWM method in which all switching devices are switched at all times within a switching cycle is widely used. Recently, many studies on the inverter efficiency improvement have been conducted. Among several switching modulation methods, the DPWM method reduces switching loss by fixing the switch state to ON or OFF for a certain time. This paper proposes a CB-DPWM method for FLI that increases the inverter system efficiency. The proposed rotation CB-DPWM method is implemented by clamping one of five pole voltages of FLI to half of DC-link voltage using the offset voltage ($V_{offset,DPWM}$).

Fig. 5 shows the voltage modulation block diagram of the proposed CB-DPWM method. The $V_{offset,DPWM}$ for proposed CB-DPWM method is calculated by using V^*_{as}, V^*_{bs}, V^*_{cs}, V^*_{ds}, and V^*_{es} of existing CB-SVPWM method. For five reference voltages of FLI, the offset voltage for the proposed CB-DPWM method should be selected so that the reference voltages limit the following:

$$0.5V_{dc} > V_{xn} \geq -0.5V_{dc}, \quad (\text{x} = \text{a,b,c,d,e}). \tag{6}$$

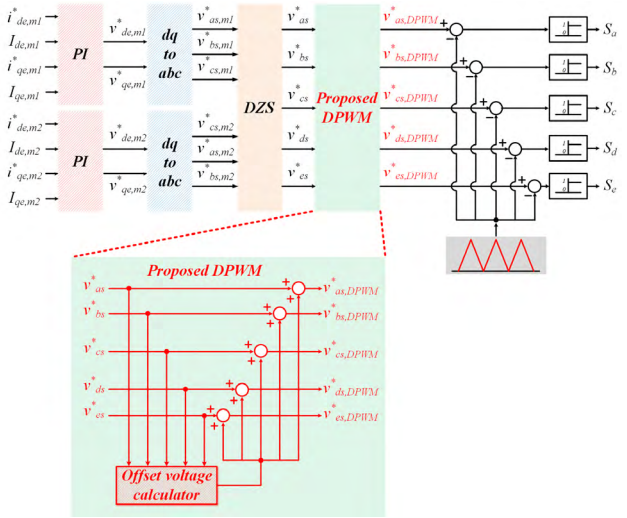

FIGURE 5. Modulation scheme using the proposed CB-DPWM method.

Therefore, the offset voltage limitation for the proposed CB-DPWM is expressed as

$$0.5V_{dc} - V_{\max,FLI} > V_{offset,DPWM} \geq -0.5V_{dc} - V_{\min,FLI}. \tag{7}$$

Since FLI has five reference voltages unlike the three-leg voltage inverter, the maximum and minimum value ($V_{max,FLI}$ and $V_{min,FLI}$) of the five reference voltages are

calculated instantaneously as

$$V_{\max,FLI} = \max\left(V_{as}, V_{bs}, V_{cs}, V_{ds}, V_{es}\right)$$
$$V_{\min,FLI} = \min\left(V_{as}, V_{bs}, V_{cs}, V_{ds}, V_{es}\right). \quad (8)$$

Using (7) and (8), the $V_{offset,DPWM}$ for proposed CB-DPWM method of FLI is calculated as

$$V_{offset,DPWM} = \begin{bmatrix} 0.5V_{dc} & -V_{\max,FLI} \\ -0.5V_{dc} & -V_{\min,FLI} \end{bmatrix}. \quad (9)$$

Fig. 6 shows the five reference voltages and the offset voltages of the FLI with the advanced speed control method. When the advanced speed control method is applied, the *C*-phase reference voltage cancels out because the phase difference of the output voltages supplied to the two induction motors is 180 degrees. In addition, the *A*- and *D*-phase reference voltage are symmetrical to each other, and *B*- and *E*-phase reference voltage are also symmetrical to each other. The offset voltage for the proposed CB-DPWM method is clamped to $0.5V_{dc}$ or $-0.5V_{dc}$, respectively, when the magnitude of each reference voltage is at its maximum or minimum. Therefore, two offset voltages for the proposed CB-DPWM are shown in (9). To apply the proposed CB-DPWM to FLI, only one of two offset voltages is used. In this case, however, one of the two switches in each leg is stressed. To address this drawback, this paper proposes the rotation CB-DPWM method as shown in Fig. 7. When the proposed rotation CB-DPWM method is applied to FLI, the final reference voltage is clamped to $0.5V_{dc}$ at the maximum value among the five reference voltages during one period of the reference voltage, and in next period of the reference voltage, the final reference voltage is clamped to $-0.5V_{dc}$ at the minimum value among the five reference voltages. Therefore, $V_{offset,DPWM}$ is expressed as

$$V_{offset,DPWM} = \begin{cases} 0.5V_{dc} - V_{\max,FLI} & (1, 3, \ldots, \textit{odd period}) \\ -0.5V_{dc} - V_{\min,FLI} & (2, 4, \ldots, \textit{even period}). \end{cases} \quad (10)$$

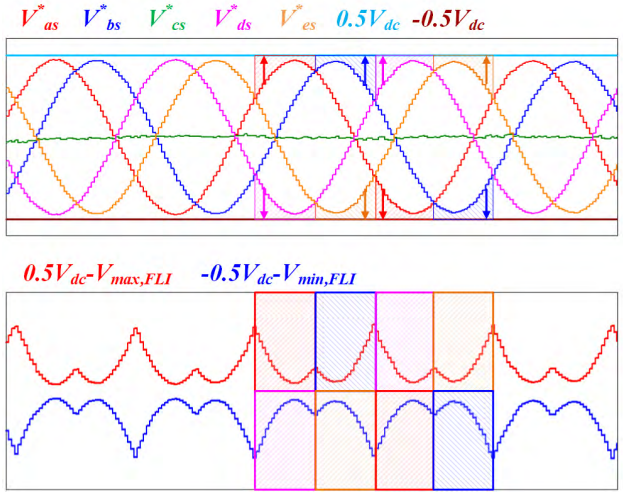

FIGURE 6. Configuration of offset voltage for proposed CB-DPWM method.

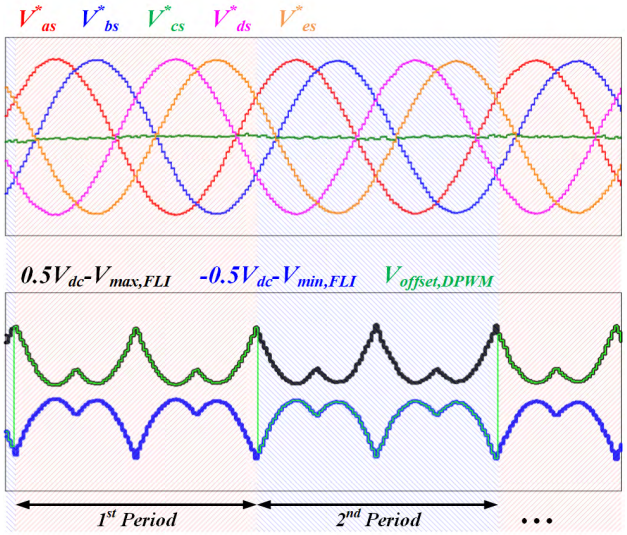

FIGURE 7. Configuration of offset voltage for proposed rotation CB-DPWM method.

Using this proposed rotation CB-DPWM method, the power distribution of the switches in each leg is balanced. Finally, by adding the $V_{offset,DPWM}$ to the five reference voltages of (5), the reference voltages ($V^*_{as,DPWM}$, $V^*_{bs,DPWM}$, $V^*_{cs,DPWM}$, $V^*_{ds,DPWM}$, and $V^*_{es,DPWM}$) of the proposed rotation CB-DPWM for FLI can be represented as

$$V^*_{as,DPWM} = V^*_{as} + V_{offset,DPWM}$$
$$V^*_{bs,DPWM} = V^*_{bs} + V_{offset,DPWM}$$
$$V^*_{cs,DPWM} = V^*_{cs} + V_{offset,DPWM}$$
$$V^*_{ds,DPWM} = V^*_{ds} + V_{offset,DPWM}$$
$$V^*_{es,DPWM} = V^*_{es} + V_{offset,DPWM}. \quad (11)$$

Fig. 8 shows the five reference voltages of the proposed rotation DPWM method in $MI_{m1} = MI_{m2} = 0.577$. For example, as shown in red dashed line in Fig. 8, during a section where V^*_{as} is the largest in negative, V^*_{as} is fixed at $-V_{dc}/2$ to keep the bottom switch of *A*-phase ON state. Similarly, as shown in blue dashed line in Fig. 8, during a section where the V^*_{ds} is the largest in positive, V^*_{ds} is fixed at $V_{dc}/2$ to keep the top switch of *D*-phase ON state. The reference voltage in the other section is changed to match the fundamental voltage. This operation is repeated based on one cycle of the reference voltage.

Fig. 9 shows the five reference voltages of the proposed rotation CB-DPWM method in $MI_{m1} = MI_{m2} = 0.35$. Comparing Fig. 8 with Fig. 9, when the *MI* decreases, $V_{offset,DPWM}$ must be large because a large clamping voltage is required for the proposed rotation CB-DPWM method. As shown in Fig. 9, the proposed rotation CB-DPWM method can be applied to FLI even if the *MI* is decreased by using five reference voltages.

Fig. 10 shows the reference voltages of the proposed rotation CB-DPWM method when the electrical angle between

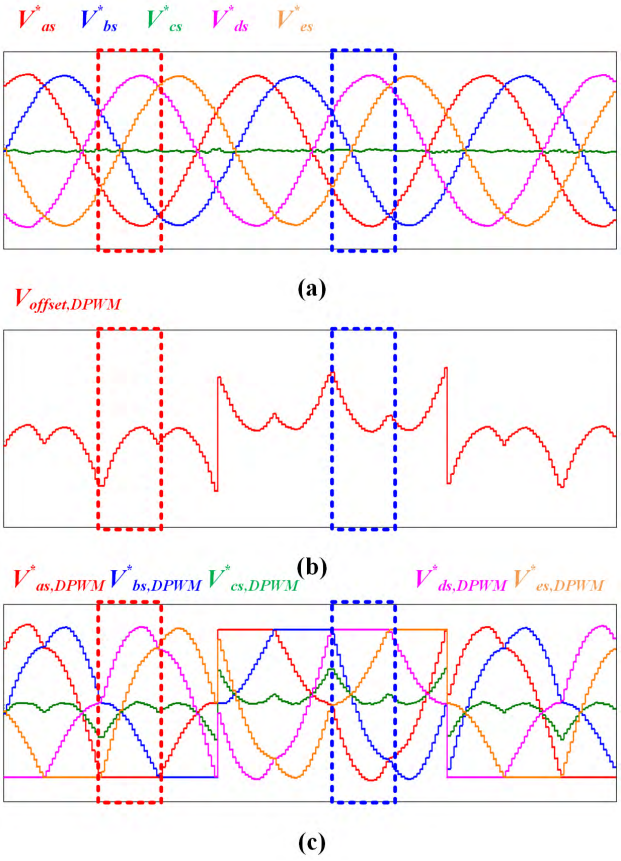

FIGURE 8. Principle of five reference voltages for the FLI (MI = 0.577). (a) Five reference voltages from DZS, (b) Offset voltage for FLI, (c) Five reference voltages for FLI.

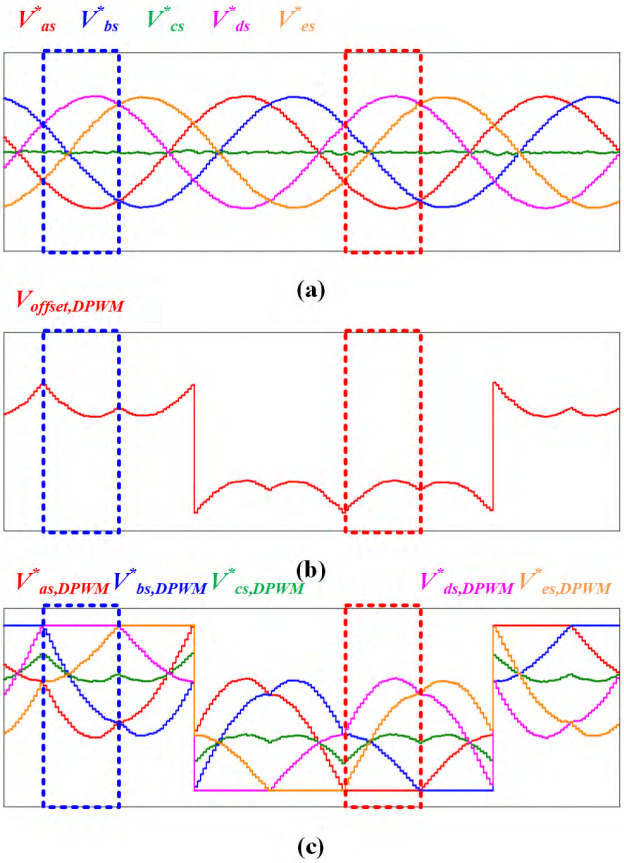

FIGURE 9. Principle of five reference voltages for the FLI (MI = 0.35). (a) Five reference voltages from DZS, (b) Offset voltage for FLI, (c) Five reference voltages for FLI.

two induction motors is 90 degrees. Similarly, the proposed rotation CB-DPWM method can be implemented using $V_{offset,DPWM}$ with different electrical angles between the two induction motors. In this case, the proposed rotation CB-DPWM method can be applied to FLI, but the current value of *C*-phase increases as described previously.

V. SIMULATION RESULTS

The simulation of FLI with proposed rotation CB-DPWM method was implemented by PSIM software to verify the operation of the proposed method. The simulation circuit is the same with Fig. 1 and the parameters of *IM1* and *IM2* are stated in Table 1. For the verification of the proposed DPWM method, the speed of two induction motors connected to FLI was controlled at 300rpm. In addition, the simulation was conducted under the same load conditions for simplicity.

Fig. 11 shows the simulation results of the reference voltage (V^*_{as}, V^*_{bs}, V^*_{cs}, V^*_{ds}, and V^*_{es}) with the CB-SVPWM ($MI_{m1} = MI_{m2} = 0.577$). As described in [24], since the angle control is applied in the advanced speed control, the phase difference between $V^*_{cs,1}$ and $V^*_{cs,2}$ is 180 degrees. Therefore, $V^*_{cs,1}$ and $V^*_{cs,2}$ cancel out each other, and V^*_{cs} is close to zero as shown in Fig. 11 and (5).

TABLE 1. Parameters for simulation and experiments.

Parameter	Value	Parameter	Value
Rated power	2.2 kW	Mutual inductance	204 mH
V_{LL}	380 V	Rotor inductance	248 mH
I_{stator}	6.6 A	Stator inductance	248 mH
Rated speed	1750 rpm	Rotor resistance	2.21 Ω
Rated torque	10 Nm	Stator resistance	1.96 Ω
P	4	V_{dc}	300 V
Moment of inertia	0.02 kgm^2	f_{sw}	10 kHz
		Sampling rate	100 μs

Fig. 12 shows the simulation results of reference voltages ($V^*_{as,DPWM}$, $V^*_{bs,DPWM}$, $V^*_{cs,DPWM}$, $V^*_{ds,DPWM}$, and $V^*_{es,DPWM}$) with the proposed rotation CB-DPWM method and the phase currents (I_a, I_b, I_c, I_d, and I_e) of FLI ($MI_{m1} = MI_{m2} = 0.577$). The proposed CB-DPWM method uses $V_{max,FLI}$ and $V_{min,FLI}$ from the five existing CB-SVPWM reference voltages to generate the offset voltage ($V_{offset,DPWM}$). In addition, two offset voltages are alternately added to the five reference voltages to balance the switching losses. Therefore, using the proposed rotation CB-DPWM method, four reference voltages except the *C*-phase reference voltage are repeatedly

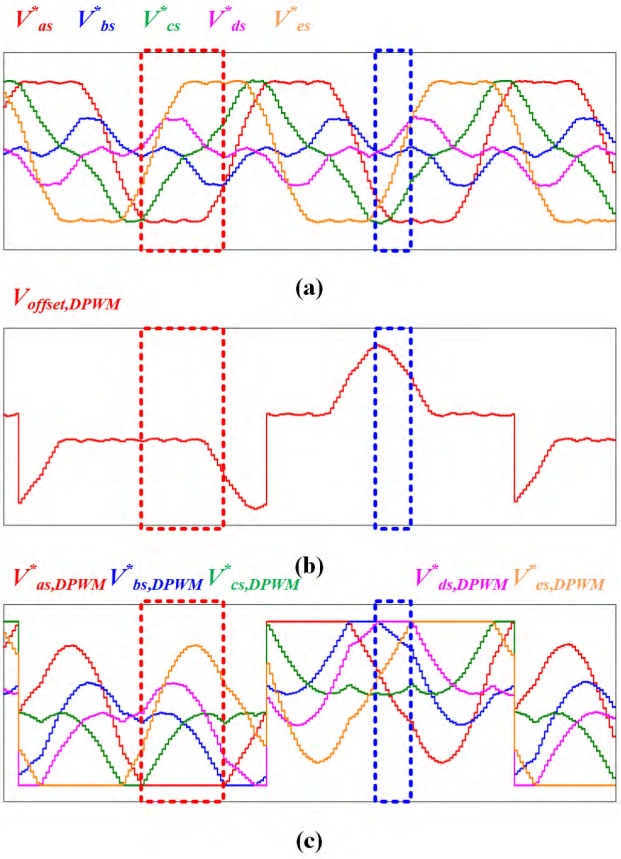

FIGURE 10. Principle of five reference voltages for the FLI without angle controller ($\alpha = 90°$). (a) Five reference voltages from DZS, (b) Offset voltage for FLI, (c) Five reference voltages for FLI.

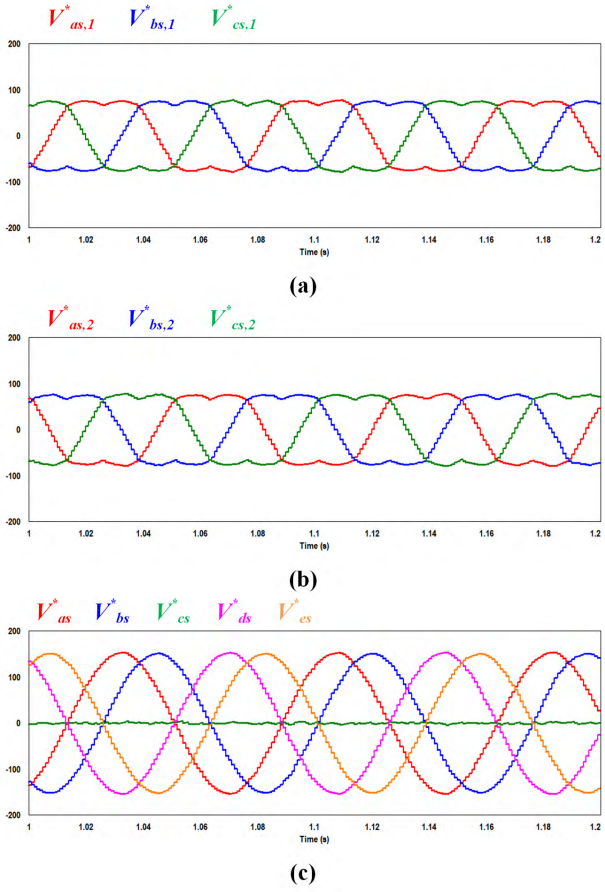

FIGURE 11. Simulation result of reference voltages with CB-SVPWM ($MI_{m1} = MI_{m2} = 0.577$). (a) Reference voltages of *M1*, (b) Reference voltages of *M2*, (c) Five reference voltages with CB-SVPWM.

clamped to $0.5V_{dc}$ or $-0.5V_{dc}$ every one period of the reference voltage. $V^*_{cs,DPWM}$ is the same shape as $V_{offset,DPWM}$ as shown in Fig. 12.

Fig. 13 and Fig. 14 show the simulation results of the pole voltages (V_{aN}, V_{bN}, V_{cN}, V_{dN}, and V_{eN}) and the phase currents with the existing CB-SVPWM method and the proposed CB-DPWM method. The pole voltage of the inverter depends on the switching operation of the switching device. As shown in Fig. 13, the pole voltages with the existing CB-SVPWM are continuous. However, the pole voltages with the proposed CB-DPWM method are discontinuous as shown in Fig. 14. In the discontinuous section, no switching loss occurs because the switching devices do not perform the switching operation. In addition, as the pole voltages of the proposed CB-DPWM method, only four of the five legs perform the switching operation. As a result, the amount of switching can be reduced by 20% compared to the existing CB-SVPWM method.

Fig. 15 shows the simulation results of advanced speed control with the proposed rotation CB-DPWM method under the variable load condition at 300 rpm. The advanced speed control, introduced in [24], ensures that both motors are electrically symmetrical and maintain the same speed despite variation of load conditions. For example, the simulation results show that when $T_{m1,load}$ decreases, the reference q-axis synchronous frame current of IM2 ($I^*_{qe,m2}$) decreases by the angle controller, and the reference d-axis synchronous frame current of IM2 ($I^*_{de,m2}$) decreases by the slip controller. In addition, FLI always operates with the proposed rotation CB-DPWM as shown in Fig. 15(d). Through the simulation results, the advanced speed control method using the proposed rotation CB-DPWM method shows that the peak current of I_c is smaller than that of the other phases in spite of variable load conditions.

VI. EXPERIMENTAL RESULTS

The experiments have been implemented using the FLI systems for the performance verification of the proposed rotation CB-DPWM method.

Fig. 16 shows the experimental set of FLI systems. The experimental set includes two induction motors, five switching device modules consisting of SKM50GB063D made by SEMIKRON, five gate drivers consisting of SKHI22BR made by SEMIKRON, two DC-link capacitors, a control board equipped with TMS320F285377D made by TI,

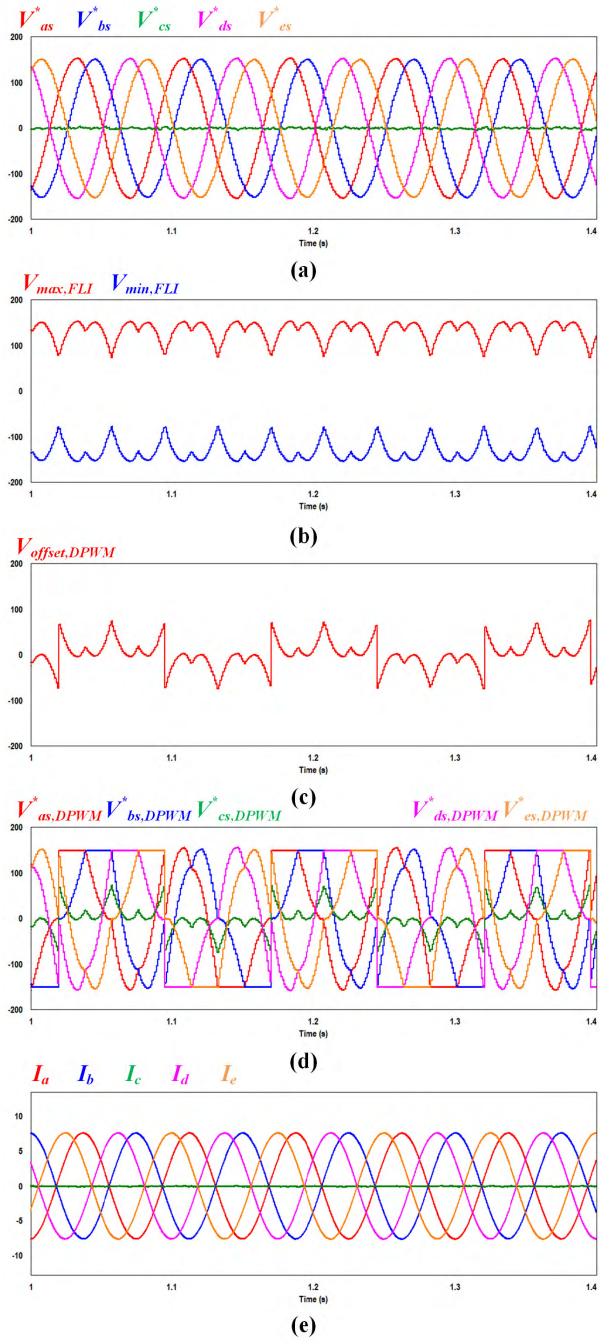

FIGURE 12. Simulation results of proposed rotation CB-DPWM ($MI_{m1} = MI_{m2} = 0.577$). (a) Five reference voltages for DZS, (b) Maximum and minimum value of five reference voltages, (c) Offset voltage for proposed CB-DPWM method, (d) Five reference voltages for proposed rotation CB-DPWM, (e) phase current of FLI.

a DC-link voltage sensor, six output current sensors, control board power supply, a DA board, two load inverter made by YASKAWA and two dynamic braking resistors. The experimental conditions were set the same as the simulation conditions in Table 1. In addition, the speed of the two induction motors connected to the FLI was controlled by the advanced speed control method at 300rpm, and the load torque of the two induction motors was set to 9Nm.

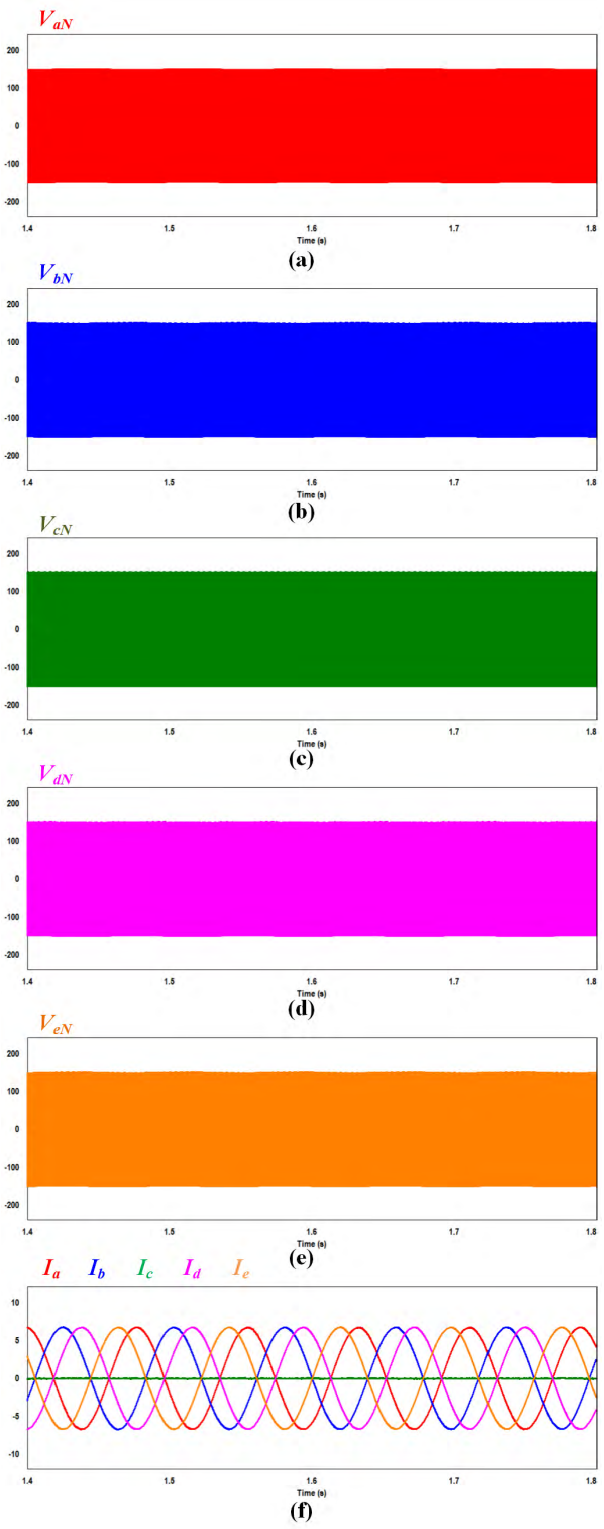

FIGURE 13. Pole voltages and phase currents of CB-SVPWM. (a) A-phase, (b) B-phase, (c) C-phase, (d) D-phase, (e) E-phase, (f) Five phase currents.

Fig. 17 shows the experimental results of five reference voltages (V^*_{as}, V^*_{bs}, V^*_{cs}, V^*_{ds}, and V^*_{es}) with existing CB-SVPWM method. The C-phase reference voltages ($V_{cs,m1}$ and $V_{cs,m2}$) of the two induction motors cancel out each

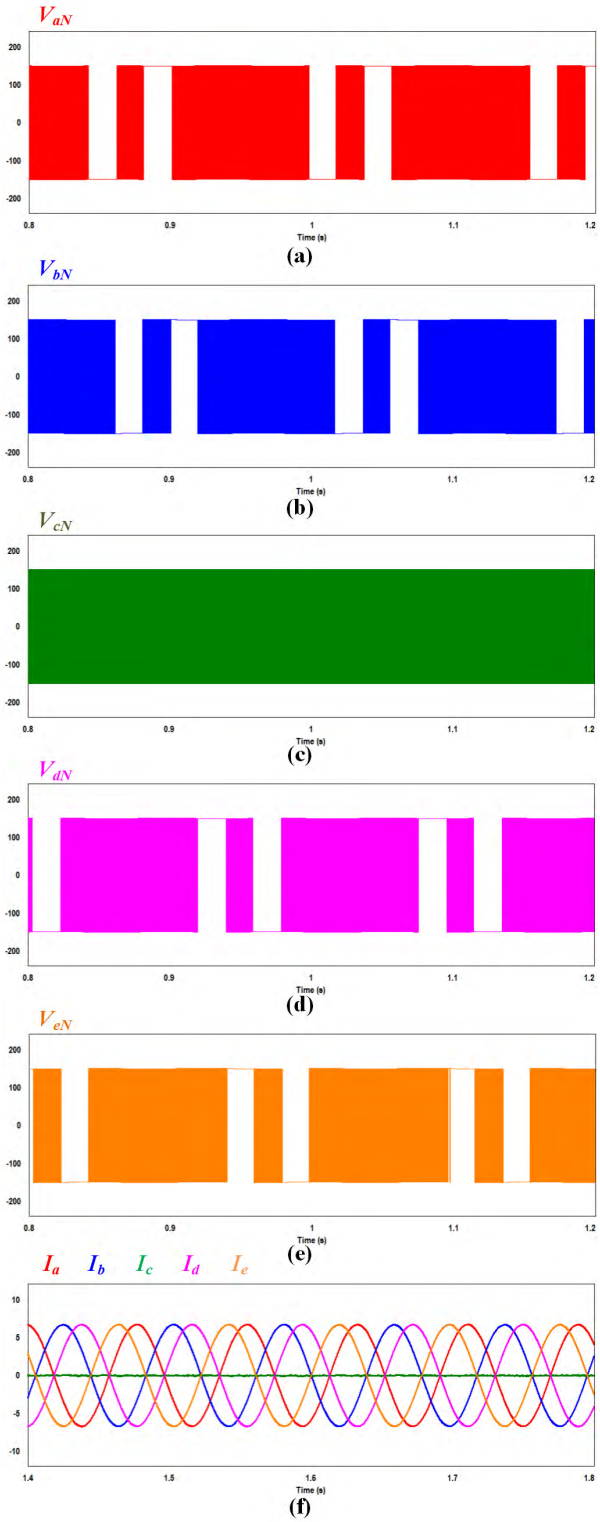

FIGURE 14. Pole voltages and phase currents of proposed rotation CB-DPWM. (a) A-phase, (b) B-phase, (c) C-phase, (d) D-phase, (e) E-phase, (f) Five phase currents.

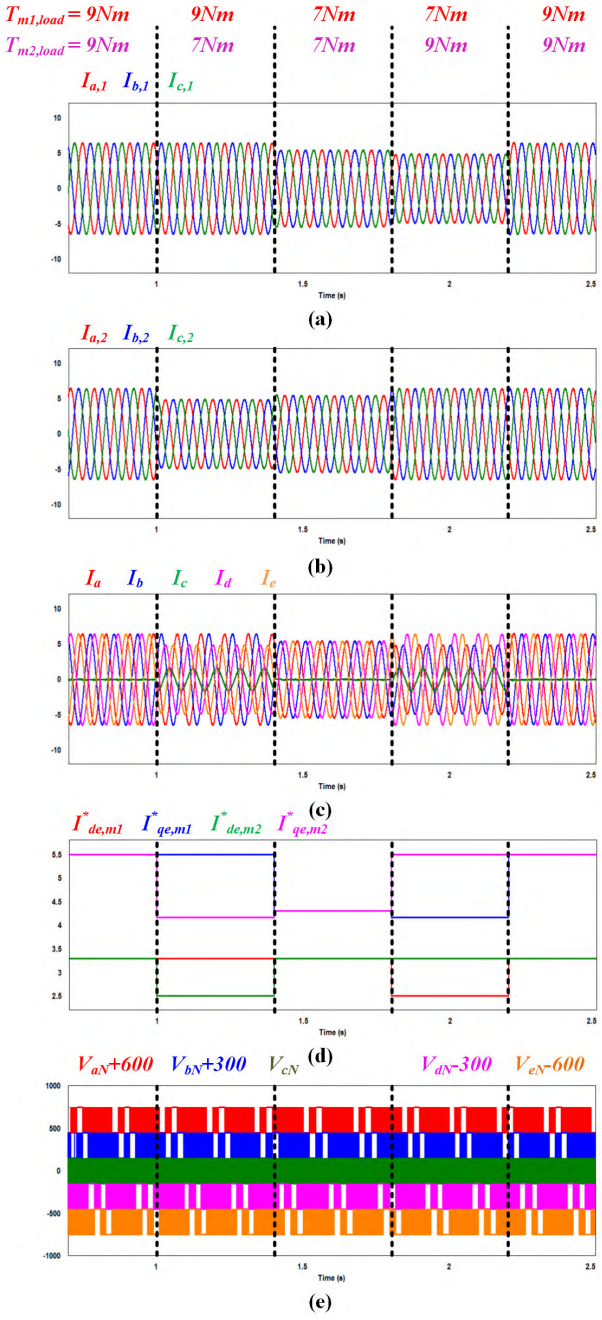

FIGURE 15. Simulation results of advanced speed control with proposed rotation CB-DPWM. (a) Phase currents of IM1, (b) Phase currents of IM2, (c) Phase currents of FLI, (d) Reference d-q axis synchronous frame current of two motors, (e) Pole voltages.

other, and the C-phase reference voltage of the FLI is close to zero due to the angle controller. However, if the load torque conditions of the two induction motors are different, the reference voltage of C-phase also appears in irregular sinusoidal waveform because the current flowing through the two induction motors is different, but it is not larger than the other phase reference voltage due to the angle controller.

Fig. 18 shows the experimental results of five reference voltages ($V^*_{as,DPWM}$, $V^*_{bs,DPWM}$, $V^*_{cs,DPWM}$, $V^*_{ds,DPWM}$, and $V^*_{es,DPWM}$) with proposed rotation CB-DPWM method.

$V_{offset,DWPM}$ is calculated using the reference voltages of the existing CB-SVPWM method, and the reference voltages

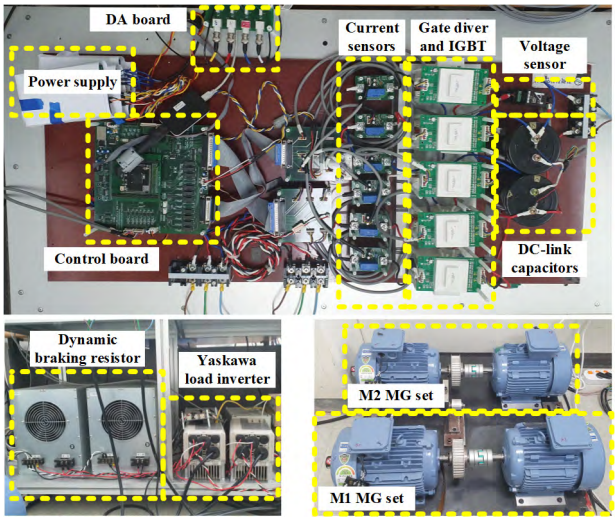

FIGURE 16. Experimental set.

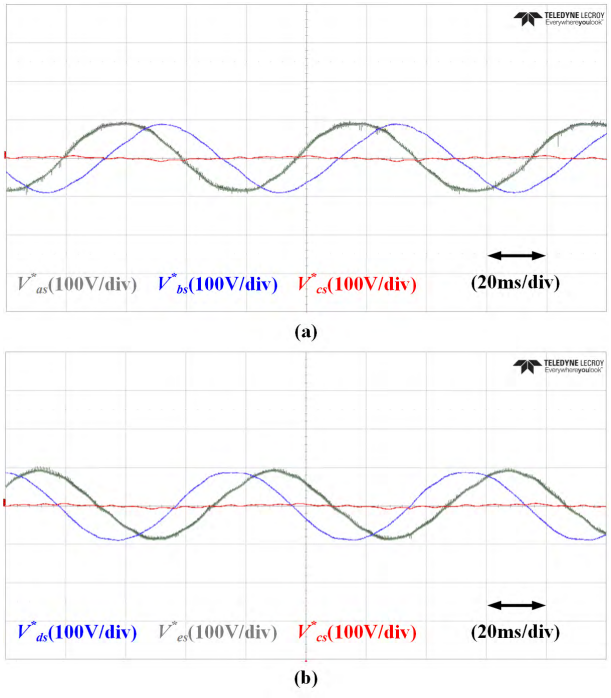

FIGURE 17. Experimental results of reference voltages with CB-SVPWM. (a) V^*_{as}, V^*_{bs}, V^*_{cs}, (b) V^*_{ds}, V^*_{es}, V^*_{cs}.

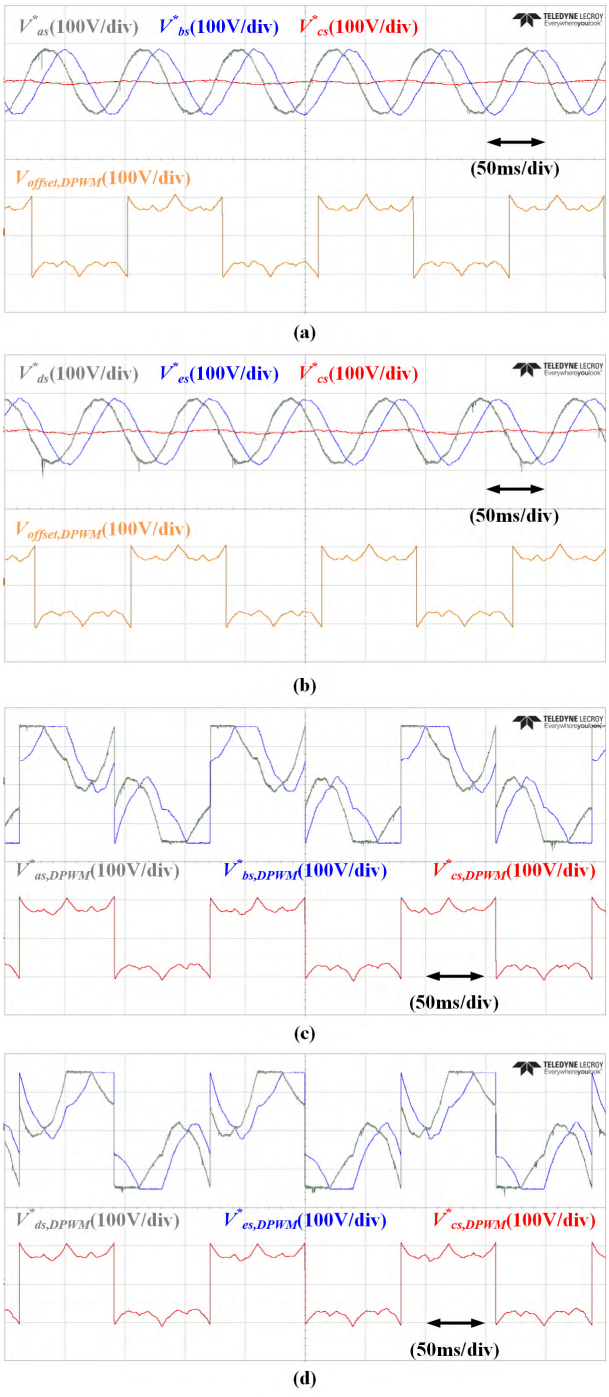

FIGURE 18. Experimental results of reference voltages with proposed rotation CB-DPWM. (a) V^*_{as}, V^*_{bs}, V^*_{cs}, $V_{offset,DPWM}$, (b) V^*_{ds}, V^*_{es}, V^*_{cs}, $V_{offset,DPWM}$, (c) $V^*_{as,DPWM}$, $V^*_{bs,DPWM}$, $V^*_{cs,DWPM}$, (d) $V^*_{ds,DPWM}$, $V^*_{es,DPWM}$, $V^*_{cs,DPWM}$.

of the proposed CB-DPWM method is generated by adding the offset voltage to the reference voltages of the existing CB-SVPWM method. In addition, the offset voltage can be used to clamp the reference voltages to $0.5V_{dc}$ or $-0.5V_{dc}$ every one period of the reference voltage as shown in Fig. 18. Therefore, when $V_{offset,DWPM}$ is added to the V^*_{xs}(x = a, b, c, d, e), it is confirmed that the clamping section for the proposed DPWM operation occurs.

Fig. 19 shows the experimental results of the pole voltages (V_{aN}, V_{bN}, V_{cN}, V_{dN}, and V_{eN}), the reference voltages, and the output currents when the proposed rotation CB-DPWM method is applied. As shown in Fig. 19, the pole voltages are discontinuous because the switching devices do not switch operation by the reference voltages. However, the C-phase switching devices always operate because the $V^*_{cs,DPWM}$ always exists between $-V_{dc}/2$ and $V_{dc}/2$.

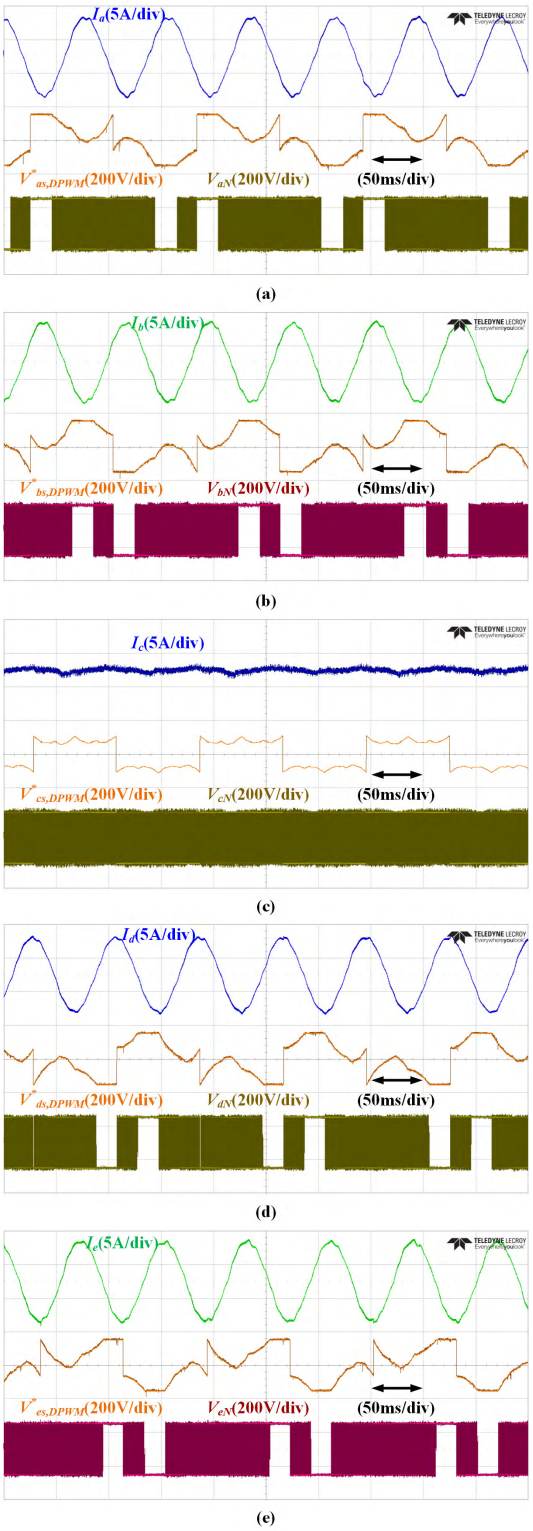

FIGURE 19. Experimental results of phase current, reference voltage, phase voltage with proposed rotation CB-DPWM. (a) A-phase, (b) B-phase, (c) C-phase, (d) D-phase, (e) E-phase.

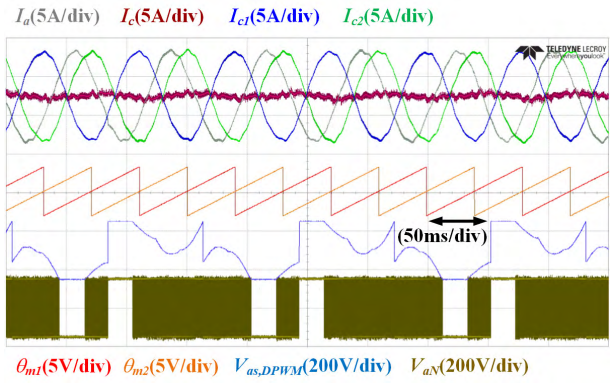

FIGURE 20. Experimental results of advanced speed control with proposed CB-DPWM.

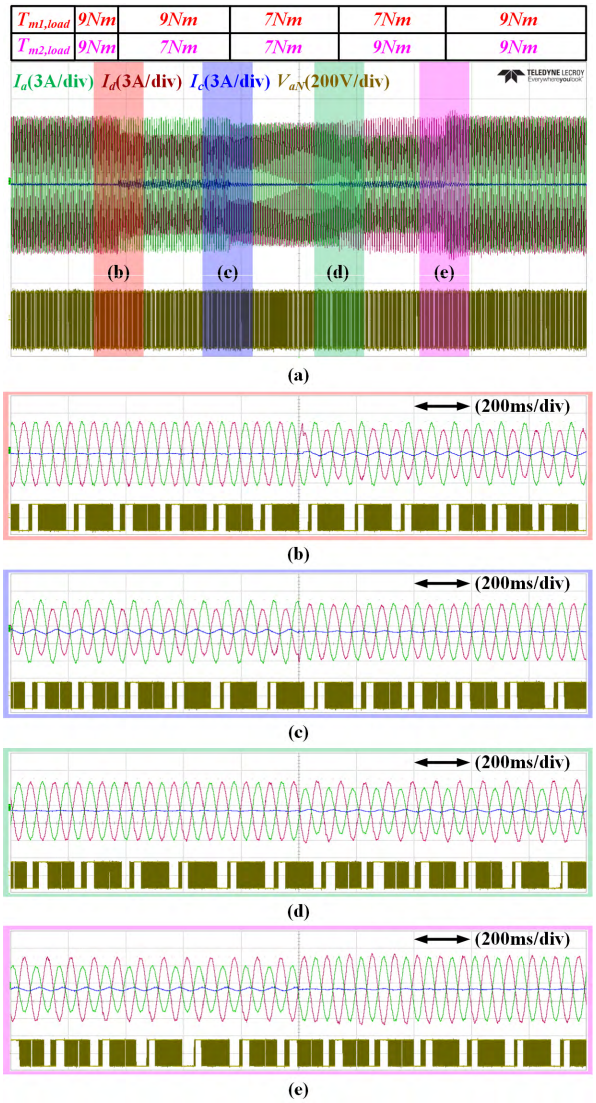

FIGURE 21. Experimental results of advanced speed control with proposed CB-DPWM under variable load condition at 300rpm.

Fig. 20 shows the experimental results of the A-phase current (I_a), the C-phase currents ($I_{c,1}$ and $I_{c,2}$) of each motor, the C-phase current (I_c) of FLI, the phase angles (θ_{m1} and θ_{m2}) of two induction motors and the A-phase pole voltage (V_{aN}). As shown in Fig. 20, even if the proposed rotation CB-DPWM method is applied to FLI, the phase angle

of *IM1* and *IM2* always differ by 180 degrees due to the angle controller, and it was confirmed that the *C*-phase current of FLI is close to zero because the $I_{c,1}$ and $I_{c,2}$ cancel out each other under the same load conditions.

Fig. 21 shows the experimental results of the advanced speed control method [24] with the proposed rotation CB-DPWM method. The load condition can be changed by applying the DC signal to the load inverter manufactured by YASKAWA. Fig. 21(b) shows the experimental results when $T_{m2,load}$ is changed from 9Nm to 7Nm. As with the simulation results in Fig. 15, $I^*_{de,m2}$ and $I^*_{qe,m2}$ are decreased by the advanced control method. In this case, the phase difference of $V^*_{cs,1}$ and $V^*_{cs,2}$ is kept symmetrical by the angle controller. However, since the magnitudes of $V^*_{cs,1}$ and $V^*_{cs,2}$ are different from each other, it can be seen that the *C*-phase current increases slightly. In addition, the *D*-phase current of FLI connected to the *A*-phase of *IM2* decreases because the load condition of *IM2* decreases. Fig. 21(c) shows the experimental results when $T_{m1,load}$ is changed from 9Nm to 7Nm. In this case, the *C*-phase current of FLI converges to zero because the load conditions of the two induction motors are the same. Fig. 21(d) and (e) show the experimental results in the opposite situation of Fig. 21(a) and (b). From V_{aN} as shown in Fig. 21, it is proved that the proposed rotation CB-DPWM method can be applied to the advanced speed control method [24] under the variable load condition.

Fig. 22 and 23 show the experimental results of the pole voltages with the existing CB-SVPWM method and the proposed rotation CB-DPWM method. As with the simulation results, the switching losses in the proposed rotation CB-DPWM method are reduced compared to the existing CB-SVPWM method because only eight of the ten switching devices operate in all switching intervals. Table 2 shows the efficiency of FLI with the existing CB-SVPWM method and the proposed rotation CB-DPWM method. The power analyzer for efficiency measurement is PX8000 made by YOKOGAWA. When the two induction motors were controlled at a constant speed, the system efficiency was measured by increasing or decreasing the load torque. As shown in Table 2, the system efficiency of FLI is always high when the proposed rotation CB-DPWM method is applied.

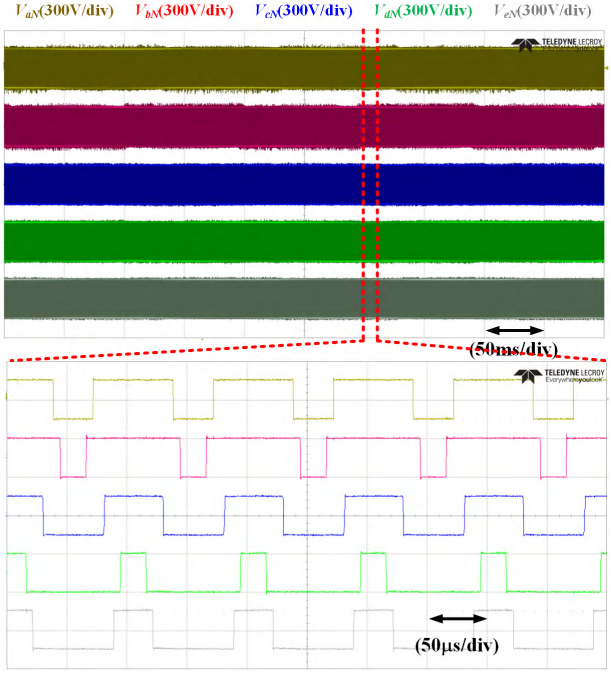

FIGURE 22. Experimental results of five phase voltage with existing CB-SVPWM.

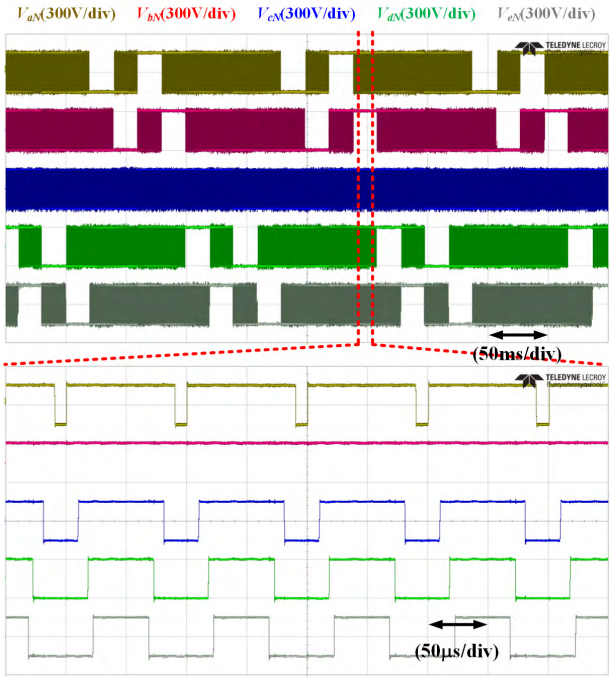

FIGURE 23. Experimental results of five phase voltage with proposed CB-DPWM.

TABLE 2. Analysis of efficiency.

CB-SVPWM	Load torque (*IM1* = *IM2*) [Nm]					
	1.5	3	4.5	6	7.5	9
I_{de} [A]	3	3	3	3	3	3
I_{qe} [A]	1	2	3	4	5	6
P_{IM1} [W]	64.1	155.3	216.9	274.6	334.9	407.6
P_{IM2} [W]	63.9	154.1	217.2	274.1	335.4	405.2
P_{Input} [W]	287.4	401.7	490.3	597.2	718.5	852.8
Efficiency [W]	44.54	77.02	88.54	91.88	93.29	95.31
CB-DPWM	**Load torque (*IM1* = *IM2*) [Nm]**					
	1.5	3	4.5	6	7.5	9
I_{de} [A]	3	3	3	3	3	3
I_{qe} [A]	1	2	3	4	5	6
P_{IM1} [W]	68.9	159.2	221.1	278.3	337.4	412.8
P_{IM2} [W]	66.7	158.2	220.2	275.2	335.2	411.9
P_{Input} [W]	278.3	388.8	489.2	589.2	715.2	851.7
Efficiency [W]	48.72	81.63	90.2	93.94	94.04	96.83

The experimental results show that the proposed rotation CB-DPWM method is about 1.5% more efficient than the existing CB-SVPWM method when the V_{dc} is 300V and the load torque with the maximum *MI* is 9Nm.

VII. CONCLUSION

In this paper, we propose a simple rotation CB-DPWM method using the offset voltage and increase the system efficiency of FLI. FLI has the advantage of being able to drive two induction motors independently by reducing the number of switching devices. By applying the proposed rotation CB-DPWM method which can reduce the number of switching device to FLI, it is possible to reduce switching loss and to balancing control of switching loss between two switches in a leg. The proposed rotation CB-DPWM method can be easily applied to hardware such as digital signal processor (DSP) because it uses the offset voltage simply calculated using the reference voltages of the existing CB-SVPWM. The experimental results show that the rotation CB-DPWM method proposed in this paper can increase the system efficiency of FLI. Therefore, by using the proposed rotation CB-DPWM method, the inverter can be made compact and it can contribute to the cost reduction of FLI. The simulation and experimental results confirm the feasibility and the effectiveness of the proposed rotation CB-DPWM method compared with the existing CB-SVPWM method.

REFERENCES

[1] M. Heydari, A. Fatemi, and A. Yazdian Varjani, "A reduced switch count three-phase AC/AC converter with six power switches: Modeling, analysis, and control," *IEEE J. Emerg. Sel. Topics Power Electron.*, vol. 5, no. 4, pp. 1720–1738, Dec. 2017.

[2] E. S. Najmi, A. H. Rajaei, M. Mohamadian, and S. M. Dehghan, "A novel dual output six switch inverter for driving two phase induction motor," in *Proc. PEDSTC*, Tehran, Iran, 2013, pp. 248–253.

[3] S. Shi, Y. Sun, M. Su, S. Xie, M. Zhou, and L. Li, "Reduced-switch induction motor drive system with active power decoupling," *IET Electr. Power Appl.*, vol. 13, no. 7, pp. 969–976, Jul. 2019.

[4] X. Li, L. Qu, B. Zhang, G. Zhang, and H. Liao, "A simplified modulation strategy of nine-switch inverter to cut off half of switching modes," *IEEE Access*, vol. 6, pp. 7254–7261, 2018.

[5] F. C. de Andrade, F. Bradaschia, L. R. Limongi, and M. C. Cavalcanti, "A reduced switching loss technique based on generalized scalar PWM for nine-switch inverters," *IEEE Trans. Ind. Electron.*, vol. 65, no. 1, pp. 38–48, Jan. 2018.

[6] M. A. Abbache, B. Tabbache, and A. Kheloui, "Direct torque control of nine switches inverter dual induction motors," in *Proc. 22nd Medit. Conf. Control Autom.*, Palermo, Italy, Jun. 2014, pp. 810–815.

[7] C. A. Reusser, "Full-electric ship propulsion, based on a dual nine-switch inverter topology for dual three-phase induction motor drive," in *Proc. IEEE Transp. Electrific. Conf. Expo (ITEC)*, Dearborn, MI, USA, Jun. 2016, pp. 1–6.

[8] Y. Lee and J.-I. Ha, "Control method for mono inverter dual parallel surface-mounted permanent-magnet synchronous machine drive system," *IEEE Trans. Ind. Electron.*, vol. 62, no. 10, pp. 6096–6107, Oct. 2015.

[9] S. Kwon and J.-I. Ha, "Fault-tolerant operation under single-phase open in mono inverter dual parallel SMPMSM with single shaft," *IEEE Trans. Power Electron.*, vol. 34, no. 12, pp. 12064–12079, Dec. 2019.

[10] T. Liu and M. Fadel, "An efficiency-optimal control method for mono-inverter dual-PMSM systems," *IEEE Trans. Ind. Appl.*, vol. 54, no. 2, pp. 1737–1745, Mar. 2018.

[11] M. Jones, E. Levi, P. Wright, S. N. Vukosavic, and D. Dujic, "Five-leg inverter PWM technique for reduced switch count two-motor constant power applications," *IET Electr. Power Appl.*, vol. 2, no. 5, pp. 275–287, Sep. 2008.

[12] W. Promkhun, V. Kinnares, K. Ohyama, and V. Thanyaphirak, "Optimal zero-sequence selection for five-leg inverter based on two-phase SVPWM fed dual two-phase induction motors," in *Proc. iEECON*, Krabi, Thailand, 2018, pp. 1–4.

[13] Y. Mei, L. Wang, L. Wang, and J. Liu, "A PWM modulation method for five-leg inverter," in *Proc. ICEMS*, Sapporo, Japan, 2012, pp. 1–4.

[14] Y. Hu, S. Huang, X. Wu, and X. Li, "Control of dual three-phase permanent magnet synchronous machine based on five-leg inverter," *IEEE Trans. Power Electron.*, vol. 34, no. 11, pp. 11071–11079, Nov. 2019.

[15] M. H. N. Talib, Z. Ibrahim, N. A. Rahim, and A. S. A. Hasim, "Implementation of space vector two-arm modulation for independent motor control drive fed by a five-leg inverter," *J. Power Electron.*, vol. 14, no. 1, pp. 115–124, Jan. 2014.

[16] J. Sabarad, G. H. Kulkarni, and S. Sattigeri, "Dual three phase induction motor control using five leg inverter," in *Proc. ICSPACE*, Bengaluru, India, 2017, pp. 120–125.

[17] C.-S. Lim, N. A. Rahim, W.-P. Hew, and E. Levi, "Model predictive control of a two-motor drive with five-leg inverter supply," *IEEE Trans. Ind. Electron.*, vol. 60, no. 1, pp. 54–65, Jan. 2013.

[18] C.-S. Lim, E. Levi, M. Jones, N. A. Rahim, and W.-P. Hew, "A comparative study of synchronous current control schemes based on FCSMPC and PI-PWM for a two-motor three-phase drive," *IEEE Trans. Ind. Electron.*, vol. 61, no. 8, pp. 3867–3878, Aug. 2014.

[19] M. Hamouda, H. F. Blanchette, and K. Al-Haddad, "A hybrid modulation scheme for dual-output five-leg indirect matrix converter," *IEEE Trans. Ind. Electron.*, vol. 63, no. 12, pp. 7299–7309, Dec. 2016.

[20] J. A. Riveros, "Pulse width modulation for asymmetrical six-phase machines fed by five-leg converters," in *Proc. IECON*, Florence, Italy, 2016, pp. 5766–5771.

[21] S. Dai, J. Wei, B. Zhou, and J. Xue, "The control strategy of open-winding permanent magnet synchronous motor drive system based on five-leg inverter," in *Proc. VPPC*, Hangzhou, China, Oct. 2016, pp. 1–5.

[22] F. Sun, M.-J. Jin, H. Hao, and J.-X. Shen, "Investigation of decoupled PWM strategy for a three-phase open-end winding permanent magnet synchronous motor using a five-leg inverter," in *Proc. IEEE VPPC*, Hangzhou, China, Oct. 2016, pp. 1–5.

[23] W. Wang, J. Zhang, and M. Cheng, "A dual-level hysteresis current control for one five-leg VSI to control two PMSMs," *IEEE Trans. Power Electron.*, vol. 32, no. 1, pp. 804–814, Jan. 2017.

[24] Y.-S. Lim, J.-S. Lee, and K.-B. Lee, "Advanced speed control for a five-leg inverter driving a dual-induction motor system," *IEEE Trans. Ind. Electron.*, vol. 66, no. 1, pp. 707–716, Jan. 2019.

[25] Q.-H. Tran and H.-H. Lee, "A new SVM method to reduce common-mode voltage of five-leg indirect matrix converter fed open-end load drives," *J. Power Electron.*, vol. 17, no. 3, pp. 641–652, May 2017.

[26] Y. Mei and S. Feng, "An optimized modulation method for a five-leg-inverter for dual induction motor drives," in *Proc. IPEMC-ECCE Asia*, Hefei, China, May 2016, pp. 660–663.

[27] U.-M. Choi, H.-H. Lee, and K.-B. Lee, "Simple neutral-point voltage control for three-level inverters using a discontinuous pulse width modulation," *IEEE Trans. Energy Convers.*, vol. 28, no. 2, pp. 434–443, Jun. 2013.

[28] J.-S. Lee and K.-B. Lee, "Performance analysis of carrier-based discontinuous PWM method for vienna rectifiers with neutral-point voltage balance," *IEEE Trans. Power Electron.*, vol. 31, no. 6, pp. 4075–4084, Jun. 2016.

[29] J.-S. Lee, R. Kwak, and K.-B. Lee, "Novel discontinuous PWM method for a single-phase three-level neutral point clamped inverter with efficiency improvement and harmonic reduction," *IEEE Trans. Power Electron.*, vol. 33, no. 11, pp. 9253–9266, Nov. 2018.

[30] A. Tcai, H.-U. Shin, and K.-B. Lee, "DC-link capacitor-current ripple reduction in DPWM-based Back-to-Back converters," *IEEE Trans. Ind. Electron.*, vol. 65, no. 3, pp. 1897–1907, Mar. 2018.

[31] C. Xia, G. Zhang, Y. Yan, X. Gu, T. Shi, and X. He, "Discontinuous space vector PWM strategy of neutral-point-clamped three-level inverters for output current ripple reduction," *IEEE Trans. Power Electron.*, vol. 32, no. 7, pp. 5109–5121, Jul. 2017.

[32] S. Bhattacharya, D. Mascarella, and G. Joos, "Space-vector-based generalized discontinuous pulse width modulation for three-level inverters operating at lower modulation indices," *IEEE J. Emerg. Sel. Topics Power Electron.*, vol. 5, no. 2, pp. 912–924, Jun. 2017.

[33] W. Jiang, J. Li, J. Wang, J. Wang, and X. Huang, "An overall minimized switching loss discontinuous PWM strategy for neutral point clamped three level inverters," *IEEE Access*, vol. 7, pp. 122387–122397, 2019.
[34] A. R. Beig, S. Kanukollu, K. Al Hosani, and A. Dekka, "Space-vector-based synchronized three-level discontinuous PWM for medium-voltage high-power VSI," *IEEE Trans. Ind. Electron.*, vol. 61, no. 8, pp. 3891–3901, Aug. 2014.
[35] Y. Bak and K.-B. Lee, "Reducing switching losses in indirect matrix converter drives: Discontinuous PWM method," *J. Power Electron.*, vol. 18, no. 5, pp. 1325–1335, Sep. 2018.
[36] M. A. Khan, A. Iqbal, S. M. Ahmad, and Z. Husain, "Analysis of discontinuous space vector PWM techniques for a seven-phase voltage source inverter," *Int. J. Power Electron. Drive Syst.*, vol. 2, no. 2, pp. 1–17, Mar. 2012.
[37] J. Prieto, M. Jones, F. Barrero, E. Levi, and S. Toral, "Comparative analysis of discontinuous and continuous PWM techniques in VSI-fed five-phase induction motor," *IEEE Trans. Ind. Electron.*, vol. 58, no. 12, pp. 5324–5335, Dec. 2011.
[38] D. Xiao, X. Li, and K. He, "Power balance of starting process for pipe belt conveyor based on master-slave control," *IEEE Access*, vol. 6, pp. 16924–16931, 2018.
[39] G. A. Christopoulos, A. Zafiris, and A. N. Safacas, "Energy savings and operation improvement of rotating cement kiln by the implementation of a unique new drive system," *IET Electr. Power Appl.*, vol. 10, no. 2, pp. 101–109, Feb. 2016.
[40] M. Gaiceanu and A. Minzararu, "Optimal control of permanent magnet synchronous machines for cold rolling mills," in *Proc. ISEEE*, Galati, Romania, 2010, pp. 105–111.
[41] A. A. S. Mohamed, A. Gopinath, and M. R. Baiju, "A simple space vector PWM generation scheme for any general *n*-level inverter," *IEEE Trans. Ind. Electron.*, vol. 56, no. 5, pp. 1649–1656, May 2009.
[42] J. H. Seo, C. H. Choi, and D. S. Hyun, "A new simplified space-vector PWM method for three-level inverters," *IEEE Trans. Power Electron.*, vol. 16, no. 4, pp. 545–550, Jul. 2001.
[43] J. Wang, Y. Gao, and W. Jiang, "A carrier-based implementation of virtual space vector modulation for neutral-point-clamped three-level inverter," *IEEE Trans. Ind. Electron.*, vol. 64, no. 12, pp. 9580–9586, Dec. 2017.

JUNE-HEE LEE (Member, IEEE) received the B.S. and Ph.D. degrees in electrical and computer engineering from Ajou University, Suwon, South Korea, in 2013 and 2018, respectively.

Since 2018, he has been with the Korea Railroad Research Institute, Uiwang, South Korea. His research interests include grid-connected systems, high-power electric machine drive, and power conversion systems.

JUNE-SEOK LEE (Member, IEEE) received the B.S., M.S., and Ph.D. degrees in electrical and computer engineering from Ajou University, Suwon, South Korea, in 2011, 2013, and 2015, respectively.

From 2015 to 2020, he was a Senior Researcher with the Propulsion System Research Team, Korea Railroad Research Institute, Uiwang, South Korea. In 2020, he joined the School of Electronics and Electrical Engineering, Dankook University, Yongin, South Korea. His research interests include high-power electric machine drives, grid-connected systems, multilevel inverter, and reliability.

JOON-HYOUNG RYU (Member, IEEE) received the B.S., M.S., and Ph.D. degrees in instrumentation engineering and electronics engineering from Ajou University, Suwon, South Korea, in 1997, 1999, and 2005, respectively.

Since 2005, he has been with the Korea Railroad Research Institute, Uiwang, South Korea. His research interests include railway propulsion systems, power electrics, and hydrogen-powered railway systems.